THE ASTROPHYSICAL JOURNAL, 533:594–600, 2000 April 20


# INTERGALACTIC $H_2$ PHOTODISSOCIATION AND THE SOFT ULTRAVIOLET BACKGROUND PRODUCED BY POPULATION III OBJECTS

BENEDETTA CIARDI,[1] ANDREA FERRARA,[2,5] AND TOM ABEL[3,4]
*Received 1998 July 9; accepted 2000 February 18*

## ABSTRACT

We study the effects of the ionizing and dissociating photons produced by Population III objects on the surrounding intergalactic medium. We find that the typical size of an $H_2$ photodissociated region, $R_d \approx 1$–5 kpc, is smaller than the mean distance between sources at $z \approx 20$–30 but larger than the ionized region by a factor depending on the detailed properties of the emission spectrum. This implies that clearing of intergalactic $H_2$ occurs before reionization of the universe is complete. In the same redshift range, the soft-UV background in the Lyman-Werner bands, when the intergalactic H and $H_2$ opacity is included, is found to be $J_{LW} \approx 10^{-30}$ to $10^{-27}$ ergs cm$^{-2}$ s$^{-1}$ Hz$^{-1}$. This value is well below the threshold required for the negative feedback of Population III objects on the subsequent galaxy formation to be effective in that redshift range.

*Subject headings:* atomic processes — cosmology: theory — galaxies: formation — intergalactic medium

## 1. INTRODUCTION

At $z \approx 1100$ the intergalactic medium (IGM) is expected to recombine and remain neutral until the first sources of ionizing radiation form and reionize it. H I reionization is essentially complete at $z \approx 5$, as it is evident by applying the Gunn–Peterson (1965) test to QSO absorption spectra. Recently, observational evidences for a patchy He II opacity of the IGM have been collected. Although somewhat controversial (see Miralda-Escudé 1997 for a discussion), such inhomogeneous He II absorption suggests an incomplete He reionization at these redshifts.

Until recently, QSOs were thought to be the main source of ionizing photons, but observational constraints suggest the existence of an early population of pregalactic objects (Population III hereafter) that could have contributed to the reheating, reionization, and metal enrichment of the IGM at high redshift. Indeed, the QSO population declines at $z \gtrsim 3$ (Warren, Hewett, & Osmer 1994; Schmidt, Schneider, & Gunn 1995; Shaver et al. 1996), and it could not be sufficient to reionize the IGM at $z \approx 5$ (Shapiro 1995 and references therein; Madau 1998). In addition, metals have been now clearly detected in Ly$\alpha$ forest clouds (Cowie et al. 1995; Tytler et al. 1995; Lu et al. 1998; Cowie & Songaila 1998), suggesting that star formation is ongoing at high redshift; finally, studies of the [Si/C] abundance ratios in low column density absorption systems (Savaglio et al. 1997), also supported by theoretical work by Giroux & Shull (1997), show that they are consistent with the presence of a softer, stellar component of the UV background.

In the following we will study the effects of the UV photons produced by massive stars in Population III objects on the surrounding IGM. In order to virialize in the potential well of dark matter halos, the gas must have a mass greater than the Jeans mass ($M_b > M_J$), which, at $z \approx 30$, is $\approx 10^5\ M_\odot$, corresponding to very low virial temperatures ($T_{vir} < 10^4$ K). To have a further collapse and fragmentation of the gas, and to ignite star formation, additional cooling is required. It is well known that in these conditions the only efficient coolant for a plasma of primordial composition, is molecular hydrogen (Peebles & Dicke 1968; Shapiro 1992, and references therein; Haiman et al. 1996; Abel et al. 1997; Tegmark et al. 1997; Ferrara 1998). As the first stars form, their photons in the energy range 11.26–13.6 eV are able to penetrate the gas and photodissociate $H_2$ molecules both in the IGM and in the nearest collapsing structures, if they can propagate that far from their source. Thus, the existence of an UV background below the Lyman limit due to Population III objects (we will refer to it as "soft-UV background", SUVB), capable of dissociating the $H_2$, could deeply influence subsequent small structure formation. Haiman, Rees, & Loeb (1997a, hereafter HRL), for example, have argued that Population III objects could depress the $H_2$ abundance in neighbor collapsing clouds, owing to their UV photodissociating radiation, thus inhibiting subsequent formation of small mass structures.

It is therefore important to assess the impact of these objects on their surroundings through detailed calculations of the various influence spheres, i.e., ionization, photodissociation, and eventually also supernova metal enriched (Ciardi & Ferrara 1997) spheres, produced by Population IIIs. This approach will provide us with an insight of the basic aspects of the topology of ionization/dissociation in the early universe; moreover, in this way we hope to be able to ultimately understand important issues as the reionization epoch and the initial stages of the galaxy formation in the universe. Obviously, the problem at hand depends crucially on the mass, radiation spectrum and formation redshift of pregalactic objects themselves. To clarify these dependences is the main aim of this paper. In practice, we study the propagation of *R*-type ionization and dissociation fronts driven into the IGM by the radiation produced by Population III massive stars in the early universe.

In § 2 we introduce the basic physical processes and give simple dimensional estimates; § 3 defines the adopted model

[1] Università degli studi di Firenze, Dipartimento di Astronomia, Largo E. Fermi 5, Firenze, Italy.
[2] Osservatorio Astrofisico di Arcetri, Largo E. Fermi 5, Firenze, Italy.
[3] Joint Institute for Laboratory Astrophysics, Campus Box 440, Boulder, CO.
[4] Laboratory for Computational Astrophysics, NCSA, University of Illinois at Urbana/Champaign, 405 N. Mathews Avenue, Urbana, IL 61801.
[5] Max-Planck-Institut für Astrophysik, Karl-Schwarzschild-Straße 1, 85748 Garching, Germany.

and the details of the radiation transfer used in the numerical work. The results and their implications are presented in § 4 and a summary in § 5 concludes the paper.

## 2. PHYSICAL PROCESSES

In this section we outline the basic physical processes underlying the problem at hand. If massive stars form in Population III objects, their photons with $h\nu > 13.6$ eV create a cosmological H II region in the surrounding IGM. Its radius, $R_i$, can be estimated by solving the following standard equation (Shapiro & Giroux 1987) for the evolution of the ionization front:

$$\frac{dR_i}{dt} - HR_i = \frac{1}{4\pi n_{\rm H} R_i^2}\left[S_i(0) - \frac{4}{3}\pi R_i^3 n_{\rm H}^2 \alpha^{(2)}\right]; \quad (1)$$

note that ionization equilibrium is implicitly assumed. $H$ is the Hubble constant, $S_i(0)$ is the ionizing photon rate, $n_{\rm H} = 8 \times 10^{-6}\Omega_b h^2(1+z)^3$ cm$^{-3}$ is the IGM hydrogen number density and $\alpha^{(2)}$ is the hydrogen recombination rate to levels $\geq 2$. First, we note that since $R_i \ll c/H$ (see eq. [2]), the cosmological expansion term $HR_i$ can be safely neglected. In its full form equation (1) has been solved by Shapiro & Giroux (1987); such solution is shown in Figure 3 and discussed later on. If steady state is assumed ($dR_i/dt \simeq 0$), then $R_i$ is approximately equal to the Strömgren (proper) radius, $R_{\rm S} = [3S_i(0)/(4\pi n_{\rm H}^2 \alpha^{(2)})]^{1/3}$. In general, $R_{\rm S}$ represents an upper limit for $R_i$, since the ionization front fills the time-varying Strömgren radius only at very high redshift, $z \approx 100$ (Shapiro & Giroux 1987). For our reference parameters it is

$$R_i \lesssim R_{\rm S} = 0.05(\Omega_b h^2)^{-2/3}(1+z)_{30}^{-2} S_{47}^{1/3} \text{ kpc}, \quad (2)$$

where $S_{47} = S_i(0)/(10^{47}$ s$^{-1})$. The comparison between $R_i$ and $R_{\rm S}$ is also shown in Figure 3; $R_s$ is typically 1.5 times larger than $R_i$ in this redshift range.

As mentioned above, in analogy with the cosmological H II region, photons in the energy range 11.26 eV $\leq h\nu \leq$ 13.6 eV, create a photodissociated sphere in the surrounding IGM. Lepp & Shull (1984) have quantified the formation of primordial molecules in the IGM after recombination. In particular, primordial $H_2$ forms with a fractional abundance of $\approx 10^{-7}$ at redshifts $\gtrsim 400$ via the $H_2^+$ formation channel. At redshifts $\lesssim 110$ when the cosmic microwave background radiation (CMB) is weak enough to allow for significant formation of $H^-$ ions, even more $H_2$ molecules can be formed. Because of the lack of molecular data, it has unfortunately not been possible to follow the details of the $H_2^+$ chemistry as its level distribution decouples from the CMB. Assuming the rotational and vibrational states of $H_2^+$ to be in equilibrium with the CMB, the $H_2^+$ photodissociation rate is much larger than the one obtained by considering only photodissociations out of the ground state. Conservatively, one concludes that these two limits constrain the $H_2$ fraction to be in the range from $10^{-6}$ to $10^{-4}$. In fact both limits have been used in the literature (see e.g., Lepp & Shull 1984; Haiman et al. 1996; Tegmark et al. 1997; Palla, Galli, & Silk 1995). In the following we will assume that the $H^-$ channel for $H_2$ formation is the dominant mechanism, i.e., that the $H_2^+$ photodissociation rate at high redshifts is close to its equilibrium value. This leads to a typical value of the primordial $H_2$ fraction of $f_{\rm H_2} \approx 210^{-6}$ (Shapiro 1992; Anninos & Norman 1996), which is found for model universes that satisfy the standard primordial nucleosynthesis constraint $\Omega_b h^2 = 0.0125$ (Copi et al. 1995), where $\Omega_b$ is the baryon density parameter and $H_0 = 100h$ km s$^{-1}$ Mpc$^{-1}$ is the Hubble constant.

On average, $f_d \approx 15\%$ of the $H_2$ molecules that are radiatively excited by photons in the Lyman-Werner (LW) bands decay to the continuum. This so called two-step Solomon process is the prime radiative $H_2$ dissociating mechanism in cosmological and interstellar environments. Recently, Draine & Bertoldi (1996) have studied this process in great detail including line overlap and UV pumping and provide simple fitting formulas to account for the self-shielding. Their treatment, however, cannot be directly applied to cosmological situations mainly because of Hubble expansion that redshifts photons out of the LW lines. We treat $H_2$ line radiation transfer in an expanding universe in detail in § 4. The optically thin rate coefficient for the two-step photodissociation process is $k_{27} = 10^8 J$ s$^{-1}$ (where $J$ is the average flux in the LW bands in units of ergs s cm$^{-2}$ Hz$^{-1}$ $-$ 1; the rate coefficients $k_i$ are labeled according to the nomenclature given in Abel et al. 1997).

The main difference between ionization and dissociation spheres evolution consists in the fact that there is no efficient mechanism to reform the destroyed $H_2$, analogous to H recombination. As a consequence, it is impossible to define a photodissociation Strömgren radius. However, given a point source that radiates $S_{\rm LW}$ photons per second in the LW bands, an estimate of the maximum radius of the $H_2$ photodissociated sphere, $R_d$, is the distance at which the (optically thin) photodissociation time ($\sim k_{27}^{-1}$) becomes longer than the Hubble time:

$$R_d \lesssim 2.5h^{-1/2}(1+z)_{30}^{-3/4} S_{\rm LW,47}^{1/2} \text{ kpc}, \quad (3)$$

where $S_{\rm LW,47} = S_{\rm LW}/(10^{47}$ s$^{-1})$. Equations (3) and (2) show that the photodissociated region is larger than the ionized region; however, even if $S_{\rm LW} \ll S_i(0)$ under most conditions $R_d$ cannot be smaller than $R_i$ since inside the H II region, $H_2$ is destroyed by direct photoionization. One might expect that these sources are able to create a SUVB, $J_{\rm LW}$, even before all primordial $H_2$ is dissociated. However, the photodissociation time of molecular hydrogen will become shorter than the Hubble time once this flux exceeds

$$J_{\rm LW}^{\rm crit} = 6.210^{-4} J_{21} h(1+z)_{30}^{3/2}, \quad (4)$$

where $J_{21} = 10^{-21}$ ergs s$^{-1}$ Hz$^{-1}$ cm$^{-2}$ sr$^{-1}$. Values of $J_{\rm LW} > J_{\rm LW}^{\rm crit}$ will lead to a substantial destruction of primordial $H_2$ and to a clearing of the universe in the LW bands.

## 3. CHEMOREACTIVE FRONTS

To substantiate the above analytical estimates we have developed a nonequilibrium multifrequency radiative transfer code to study the detailed structure of $R$-type ionization and dissociation fronts surrounding a point source. We have adopted a standard CDM model ($\Omega_m = 1$ and $h = 0.5$, $\sigma_8 = 0.6$), with a baryon density parameter $\Omega_b = 0.06\Omega_{b,6}$, of which a fraction $f_b \sim 0.08 f_{b,8}$ (Abel et al. 1997) is able to cool and become available to form stars. We study the evolution of ionization and dissociation fronts due to photons with energy $h\nu > 13.6$ eV and 11.26 eV $< h\nu <$ 13.6 eV, respectively, produced by a point source of baryonic mass $M_b = \Omega_b M \sim 10^5\ M_\odot$ ($M = 10^6 M_6\ M_\odot$ is the total mass of the object) forming at redshift $z = 30$. The program evolves the energy equation (see, for example, Shapiro, Giroux, & Babul 1994; Ferrara & Giallongo 1996) and the chemical network equations (Abel et al. 1997), including 27

chemical processes and nine species (H, $H^-$, $H^+$, He, $He^+$, $He^{++}$, $H_2$, $H_2^+$ and free electrons). The chemical abundances are initialized according to the estimates provided by Anninos & Norman (1996). The cooling model includes collisional ionization, recombination, collisional excitation and bremsstrahlung cooling of atomic hydrogen and helium, molecular hydrogen cooling, Compton cooling on the CMB, cosmological expansion cooling and all relevant heating mechanisms (i.e., photoionization and photodissociation of all species).

### 3.1. *UV Photon Production*

We now estimate the UV photon production in protogalactic objects. We assume that the total ionizing photon rate is proportional to the baryonic mass $M_b$:

$$S_i(0) = \frac{M_b}{m_p\, t_{\rm OB}\, \tau}\, f_{\rm uvpp}\, f_{\rm esc}\, f_b \approx 10^{47} f_{\rm uvpp,48}\, f_{\rm esc,20}\, \Omega_{b,6}\, f_{b,8}\, M_6\, {\rm s}^{-1}\,, \quad (5)$$

where $t_{\rm OB} \approx 310^7$ yr is the average lifetime of massive stars; $f_{\rm uvpp} \approx 48000 f_{\rm uvpp,48}$ is the number of UV photons produced per collapsed proton (Tegmark, Silk, & Blanchard 1994); $f_{\rm esc} \approx 0.2 f_{\rm esc,20}$ is the photon escape fraction from the protogalaxy; and $\tau^{-1} \approx 0.6\%$ is the star formation efficiency, normalized to the Milky Way. This simple estimate is within a factor of 2 of the value obtained from the recently revised version of the Bruzual & Charlot (1993, hereafter BC) spectrophotometric code using a Salpeter IMF, a burst of star formation, and a metallicity $Z = 10^{-2}\, Z_\odot$. The adopted reference value $f_{\rm esc} = 0.2$ is an upper limit derived from observational (Leitherer et al. 1995; Hurwitz, Jelinsky, & Dixon 1997) and theoretical (Dove & Shull 1994) studies.

As a start, we have assumed a simple power-law spectrum above the Lyman limit and a flux with constant intensity for photons with energies lower than 13.6 eV:

$$j(\nu) = \begin{cases} j_0 \left(\dfrac{\nu}{\nu_L}\right)^{-\alpha} & 13.6\ {\rm eV} < h\nu < 850\ {\rm eV}\,, \\ \beta j_0 & h\nu < 13.6\ {\rm eV}\,, \end{cases} \quad (6)$$

where $\alpha = 1.5$ (see § 4 for a discussion on $\alpha$), and $j_0 = S_i(0) h/\alpha$ ergs$^{-1}$ Hz$^{-1}$ is the source luminosity per unit frequency; $\beta = j(13.6^-)/j(13.6^+)$ is the ratio between the flux just below and above the Lyman limit. The precise value of $\beta$ is rather uncertain and can be estimated from the results of spectrophotometric synthesis codes; in particular, we have used the BC code. We find that during most of the evolution of the stellar cluster the value of $\beta$ remains close to 1; however, in the late evolutionary stages, after the massive stars producing the ionizing flux have died, $\beta$ increases up to $\approx 30$ (although in absolute value the dissociating flux has decreased) since the dissociating photons are partly produced by the remaining intermediate-mass stars. For this reason, the value of $\beta$ is somewhat dependent on the adopted IMF (throughout the paper we use a Salpeter IMF), which determines the relative number of intermediate-to-massive stars.

### 3.2. *Radiative Transfer*

The radiative transfer equation in an expanding universe is

$$\frac{1}{c}\frac{\partial J_\nu}{\partial t} + \frac{1}{a}\frac{\partial J_\nu}{\partial R} - \frac{H}{c}\left(\frac{\partial J_\nu}{\partial \nu}\,\nu - 3J_\nu\right) = \epsilon_\nu - \kappa_\nu J_\nu\,, \quad (7)$$

where $J_\nu(r) = j(\nu)/R^2$ (ergs s$^{-1}$ cm$^{-2}$ Hz$^{-1}$); $a = (1 + z_{\rm em})/(1 + z_{\rm abs}) \sim 1$, with $z_{\rm em}$ and $z_{\rm abs}$ emission and absorption redshift, respectively. As the scales of interest are small, equation (7) can be used in the local approximation, i.e., we can neglect the cosmological redshift and the time-dependent terms; $\epsilon_\nu$(ergs$^{-1}$ cm$^{-3}$ Hz$^{-1}$), the emissivity of the gas, can be neglected when using the canonical "on the spot approximation" (cf. Osterbrock 1989); and $\kappa_\nu$(cm$^{-1}$), the frequency-dependent absorption coefficient, is implicitly assumed to vary on timescales larger then the photon crossing time. Under these approximations, equation (7) reduces to:

$$\frac{\partial J_\nu}{\partial R} = -\kappa_\nu J_\nu\,. \quad (8)$$

In the expression for $\kappa_\nu = \sum_i \sigma_i n_i$, with $\sigma_i$ (cm$^2$) and $n_i$ [cm$^{-3}$], respectively, the cross section and number density of species $i$, we have included the contribution of all the relevant species.

## 4. RESULTS AND IMPLICATIONS

Using the above assumptions, we have derived the redshift evolution of the IGM temperature and chemical abundances as a function of distance $R$ from the central source, which is supposed to turn on at $z = 30$.

In Figure 1 we show these results for the specific value of the parameter $\beta = 1$ (see eq. [6]), which should appropriately describe the radiation spectrum in the early stages of the evolution of the Population III stellar cluster, as discussed in § 3; Figure 2 illustrates the analogous temperature evolution (which is independent on the value of $\beta$, since photodissociation is negligible with respect to photoionization in terms of heating). For a comparison with previous works, see for example Shapiro, Giroux, & Kang (1987).

The location of the ionization and dissociation fronts, moving away from the central radiation source, is clearly identified by the sudden drop in the ionized hydrogen and raise of the molecular hydrogen abundance, respectively. As

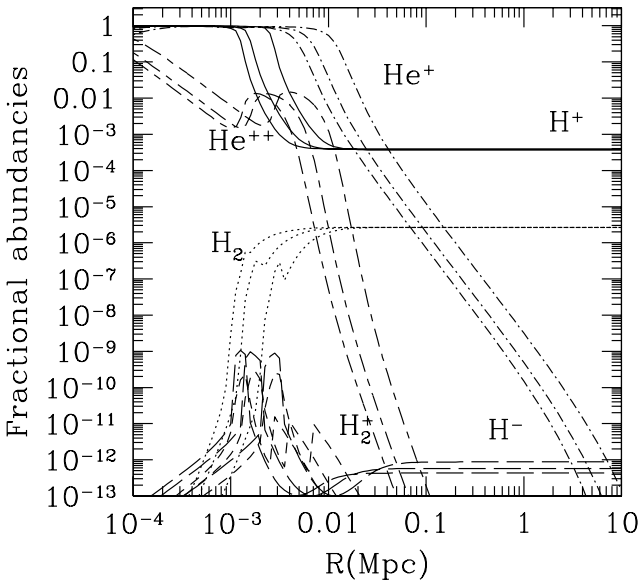


FIG. 1.—Evolution of chemical abundances as a function of distance from a Population III of total mass $M \approx 10^6\, M_\odot$, turning on at $z \approx 30$. From left to right the curves refer to $z = 27$, 23, and 19.

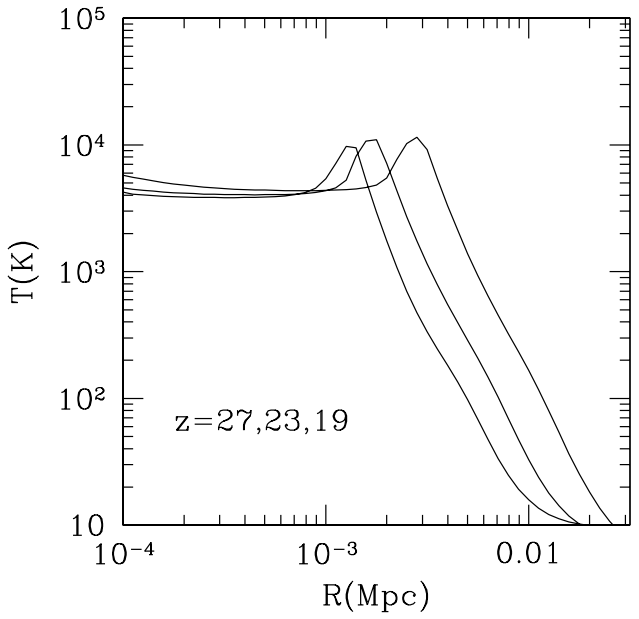


FIG. 2.—Evolution of gas temperature as a function of distance from a Population III of total mass $M \approx 10^6\ M_\odot$, turning on at $z \approx 30$. From left to right the curves refer to $z = 27$, 23, and 19.

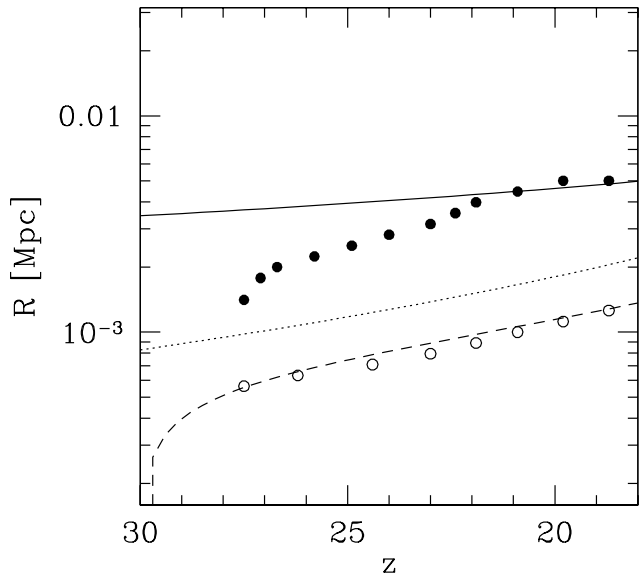


FIG. 3.—Ionization radius, $R_i$ (*open circles*) and photodissociation radius, $R_d$ (*filled circles*) of the regions produced by a Population III of total mass $M \approx 10^6\ M_\odot$, turning on at $z \approx 30$, as a function of redshift. Also shown is the maximum radius of the dissociated region (*solid line*), given by eq. (3), the Strömgren radius $R_S$ (*dotted line*), given by eq. (2), and the solution of eq. (1) (*dashed line*).

the dissociating flux is diluted at large $R$, the $H_2$ abundance reaches its asymptotic value, given by the IGM relic fraction at recombination $\approx 2 \times 10^{-6}$. In addition, the He singly ionized region is also shown to be larger than the H one, a well-known effect produced by the penetrating high-energy photons of the power-law radiation spectrum. A similar feature is not seen in $He^+$ ionization owing to the paucity of photons capable to ionize such a species. Inside the dissociated sphere, $H_2$ is basically completely destroyed by the two-step Solomon process and by ionization. $H^-$ and $H_2^+$ ions abundances have a peak at the same location as the temperature bump (see Fig. 2); this temperature increase, together with the persisting large supply of free electrons, favors the formation rate of the above species; nevertheless, the $H_2$ formation rate is completely negligible. The temperature (Fig. 2) inside the ionized region is roughly constant and equal to $\approx 10^4$ K; the small bump in the temperature profile is due to the decrease in the number of electrons responsible for collisional excitation of atomic cooling lines, in turn due to the decrease of the ionizing flux. The shape of the curves depends on the choice of the flux power-law index, $\alpha$: in addition to the standard case $\alpha = 1.5$, we have also run the case of softer spectra, $\alpha = 5$. In this case the H ionization transition region becomes steeper and the He ionized regions are shrunken. These differences are, however, not particularly relevant to the main focus of this paper, since the $H_2$ abundance is not sensibly affected.

In addition to the case $\beta = 1$ we have also run cases with $\beta$ varying in the range 1–100, finding that the above general considerations remain essentially unchanged. The only important change is represented by the absolute and relative values of the dissociation, $R_d$, and ionization, $R_i$, radii, that we are discussing next. Practically, we have defined $R_i$ and $R_d$ as the radius at which the ionized fraction deviates from unity and the $H_2$ fraction differs from its asymptotic value by less than an arbitrary constant $p \approx$ few percent, respectively. This choice leads to a good agreement with the analytical solution of equation (1) for $R_i$. In Fig. 3 we plot the numerical values of $R_i$ and $R_d$ as function of redshift, for $\beta = 1$. Equation (3) with $S_{\rm LW} = \beta S_i(0)$ gives a simple estimate for the asymptotic value of $R_d$. This limiting value is reached after about one photodissociation time $t_d$. For $\beta = 1$ it is $R_d \simeq 3.5 R_i$, while for higher values of $\beta$, $R_d$ becomes much larger than $R_i$, because of the increased number of LW photons. This roughly agrees with the estimate obtained by taking the ratio of the two radii from equations (3) and (2):

$$\frac{R_d}{R_i} = 6 h^{5/6} \Omega_{b,6}^{2/3} (1+z)_{30}^{5/4} \beta^{1/2} S_{47}^{1/6} \ . \qquad (9)$$

Since $H_2$ inside the ionized region is always destroyed via direct photoionization, by definition it must be $R_d \geq R_i$; then equation (9) holds down to a redshift $1 + z \approx 7 h^{-2/3} \Omega_{b,6}^{-8/15} \beta^{-2/5} S_{47}^{-2/15}$. As we will see, it is important to compare the size of the dissociated regions around Population III objects with their average interdistance, $d$, to determine if the surviving intergalactic $H_2$ can build up a nonnegligible optical depth to LW photons. The proper number density distribution, $n(v_c, z)$, of dark matter halos as function of their circular velocity, $v_c$, and redshift can be computed by using the Press-Schechter formalism (Press & Schechter 1974; for a modern formulation see, for example, White & Frenk 1991 and Bond et al. 1991). For the adopted CDM model such distribution is shown in Fig. 4 for the values $v_c = 7$ km s$^{-1}$ (15 km s$^{-1}$), that correspond to a mass $M \approx 10^6\ M_\odot$ ($10^7\ M_\odot$) in the redshift interval 20–30. Also shown is the evolution of the typical interdistance between such objects, $d(z) \simeq [n(v_c, z)]^{-1/3}$. We find that the mean distance between Population III objects in the relevant redshift range is equal to 0.01–1 Mpc. As $d$ is bigger than the typical derived size of $H_2$ regions at these redshifts (see eq. [3]), the $H_2$ regions can hardly overlap and completely destroy the primordial $H_2$ molecules. From these simple

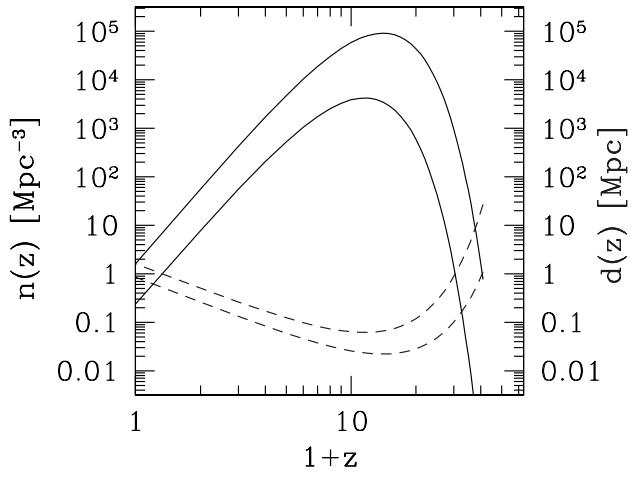


FIG. 4.—Evolution of the proper number density $n(z)$ (*solid lines*) and typical interdistance $d(z)$ (*dashed lines*) of dark matter halos with circular velocity $v_c \approx 7$ km s$^{-1}$ (*upper solid line* and *lower dashed line*) and $\approx 15$ km s$^{-1}$ (*lower solid line* and *upper dashed line*), corresponding to mass $M \approx 10^6$ $M_\odot$ and $\approx 10^7$ $M_\odot$, respectively, in the redshift range of interest 20–30, in a $\sigma_8 = 0.6$ CDM model.

considerations, one can conclude that $H_2$ photodissociated sphere overlapping will become important at $z \lesssim 20$. This finding is also supported by numerical simulations that will be presented in a forthcoming communication. Note that equation (9) also implies that clearing of intergalactic $H_2$ occurs before reionization of the universe is complete.

### 4.1. *Soft-UV Background*

In the redshift range 20–30, before overlapping becomes substantial, a SUVB will be present. To derive the intensity of the SUVB, $J_{\rm LW}$, we assume that the filling factor of the dissociated regions is small, as it follows from the inequality $R_d \ll d$. In order to evaluate the SUVB properly including the intergalactic $H_2$ attenuation, the effects of cosmological expansion must be taken into account. To this aim it is necessary to make a detailed treatment of the radiative transfer through LW $H_2$ lines. LW lines are optically thin in the redshift range of interest, with $\tau_i = N_{{\rm H}_2,i}\,\sigma_i \sim 0.05$, essentially for all the lines. This implies that as $J_{\rm LW}$ is redshifted as a result of the cosmological expansion, it is attenuated by each LW line encountered by a factor $e^{-\tau_i}$. Also, for an IGM temperature of about 10 K (adiabatic expansion can make the neutral, post recombination IGM cooler than the CMB), the Doppler line width is $\sim 1.25 \times 10^{-5}$ eV, thus implying that line overlapping can be safely neglected. Abgrall & Roueff (1989) have included in their study of classic $H_2$ PDRs more than 1000 LW lines. As in our case, $H_2$ formation that leaves the molecule in excited rovibrational levels, is negligible, a smaller number of lines $\approx 70$—involving the ground state only—needs to be considered. Globally, $J_{\rm LW}$ is attenuated by a factor $e^{-\tau_{{\rm H}_2}}$, where $\tau_{{\rm H}_2} = \sum_i \tau_i$, and $i$ runs up to the 71 lines considered from the ground rovibrational states; we obtain a $\tau_{{\rm H}_2} \lesssim 3$, depending on the number of lines encountered, and thus on the photon energy. In general, one can thus derive the intensity of the background as

$$J_{\rm LW}(\nu, z) = c \int_{z_{\rm on}}^{z} \epsilon(\nu', z') e^{-\tau_{{\rm H}_2}(\nu', z')} \frac{(1+z)^3}{(1+z')^3} \left| \frac{dt}{dz'} \right| dz' , \quad (10)$$

$$\epsilon(\nu', z') = \int_{v_{\rm min}}^{v_{\rm max}} j(\nu') \mathcal{N}(v_c, z') dv_c , \quad (11)$$

where $z_{\rm on} = 30$, $v_{\rm min} = 7$ km s$^{-1}$, $v_{\rm max} = 15$ km s$^{-1}$, $\nu' = \nu(1+z')/(1+z)$; $\epsilon(\nu', z')$ (ergs cm$^{-3}$ s$^{-1}$ Hz$^{-1}$) is the proper emissivity due to sources with $v_{\rm min} \le v_c \le v_{\rm max}$, corresponding to objects in which $H_2$ cooling is dominant; $j(\nu')$ is given in equation (6); and $\mathcal{N}(v_c, z')$ is the source number density in the velocity interval $dv_c$. The value of $J_{\rm LW}$ is not sensitive to different choices of $v_{\rm max}$, as there are very few bound structures with $v_c > v_{\rm max}$ in the redshift range of interest; on the other hand, lower values of $v_{\rm min}$ have little effect on $J_{\rm LW}$, owing to the faintness of these low-mass objects.

In Figure 5 the spectrum of the SUVB at $z = 27$ is shown, for different choices of the baryon cooling efficiency $f_b = 0.08$, 1 (which in turn implies different $j_0$ values) and in which the IGM LW attenuation is either included or neglected for comparison sake. As $J_{\rm LW}$ depends linearly on $\beta$, the results for different values of $\beta$ can be easily obtained by appropriately scaling the plotted curves. From Figure 5 we see that the intergalactic $H_2$ absorption decreases the SUVB intensity by approximately 30%.

In addition to the LW absorption lines, we have also investigated the relative importance of the neutral H lines absorption in the calculation of $J_{\rm LW}$, in analogy with the study of HRL. In Figure 6 we compare the effect of such lines and $H_2$ lines on the SUVB attenuation, for a typical choice of the parameters. The H lines are optically thick at their center; this, combined with the effect of the cosmological expansion, produces the typical sawtooth modulation of the spectrum. On the other hand, the radiative decay of the excited H atoms produces Ly$\alpha$ and other Balmer or lower line photons, which are out of the LW energy range and result in an increase of the flux just below the Ly$\alpha$ frequency. From Figure 6 we see that the H line attenuation dominates on the $H_2$ one over the all range of frequencies,

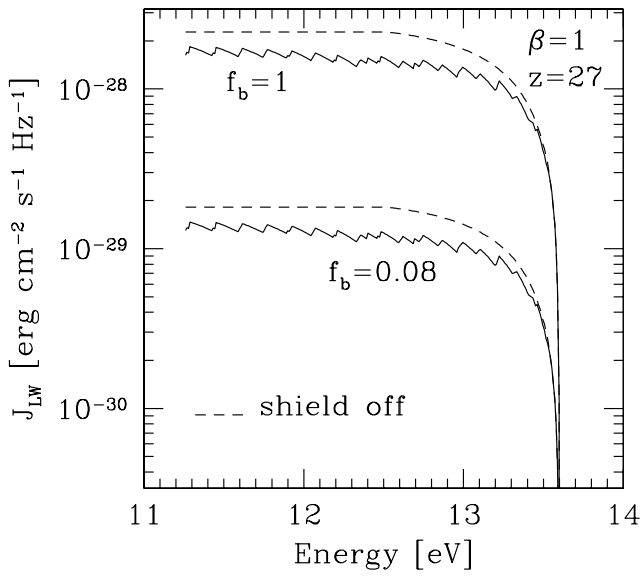


FIG. 5.—Spectrum of the SUVB, $J_{\rm LW}$, for $z = 27$, $\beta = 1$ and for baryon cooling efficiency $f_b = 0.08,1$; the intergalactic $H_2$ Lyman-Werner opacity is either included (*solid lines*) or neglected (*dashed lines*).

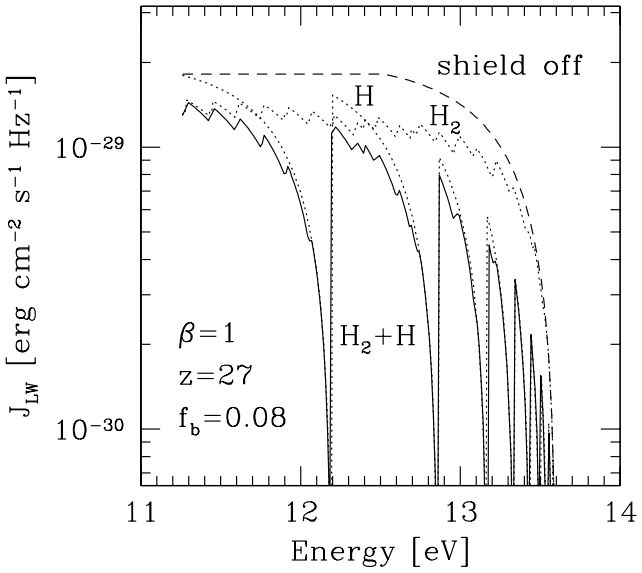


FIG. 6.—Same as Fig. 5, but for the particular values $z = 27$, $\beta = 1$ and baryon cooling efficiency $f_b = 0.08$; a comparison is shown between four different prescriptions for the intergalactic attenuation: no shielding (*dashed line*), neutral H lines opacity only (*dotted line*), $H_2$ lines opacity only (*dotted line*), and the sum of $H_2$ and neutral H lines opacity (*solid line*).

except from the limited spectral regions blueward of the Ly$\beta$ and Ly$\gamma$ resonances.

The evolution of $J_{LW}$ with $z$ is shown in Figure 7, for $\langle h\nu \rangle = 12.45$ eV, the central frequency of the LW band.

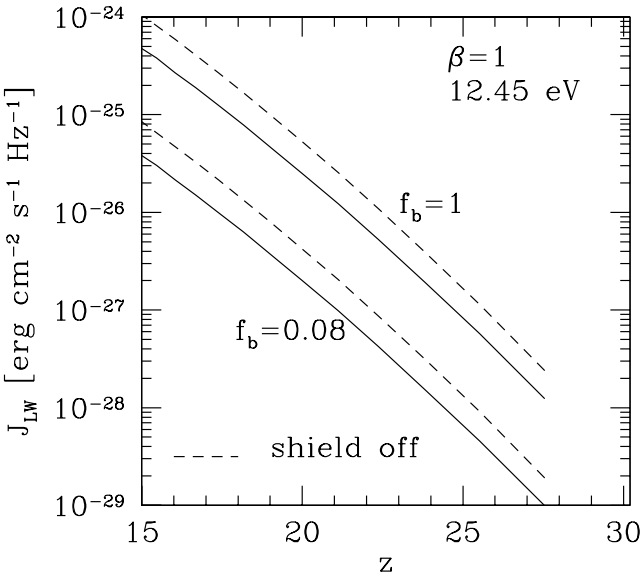


FIG. 7.—Evolution with redshift of the SUVB, $J_{LW}$, for $h\nu = 12.45$ eV, $\beta = 1$ and for baryon cooling efficiency $f_b = 0.08,1$; the intergalactic H lines and $H_2$ Lyman-Werner opacity is either included (*solid lines*) or neglected (*dashed lines*).

From the plot we see that typically, a SUVB intensity $J_{LW} \approx 10^{-30}$ to $10^{-26}$ ergs cm$^{-2}$ s$^{-1}$ Hz$^{-1}$ is produced by Population III objects.

These results are particularly important when the effects of the possible "negative feedback" are to be considered. HRL concluded that in principle a SUVB created by pregalactic objects, would be able to penetrate large clouds, and, by suppressing their $H_2$ abundance, prevent the collapse of the gas. One of their conclusions (Haiman et al. 1997b) is that in the redshift range $z = 25$–$35$, a minimum SUVB intensity, $J_{LW} \approx 10^{-24}$ ergs cm$^{-2}$ s$^{-1}$ Hz$^{-1}$ is required to significantly affect or inhibit the collapse of forming objects. From Figure 7 we conclude that at these redshifts the intensity of the SUVB is well below the threshold required for the negative feedback of Population III objects on the subsequent galaxy formation to be effective. Clearly, if at redshift $\approx 20$ complete overlapping of photodissociated regions occurs, as previously suggested, the SUVB intensity can be increased to interesting values for negative feedback effects. However, by that time a considerable fraction of the objects in the universe that must rely on $H_2$ cooling (i.e., $v_c \lesssim 15$ km s$^{-1}$) for collapse might be already in an advanced evolutionary stage (see Fig. 4) and actively forming stars. It follows that negative feedback can at best only partially influence the formation of small objects. To confirm this hypothesis, that depends on the details of structure formation, numerical simulations are required.

## 5. SUMMARY

We have studied the evolution of ionization and dissociation spheres produced by and surrounding Population III objects, which are supposed to have total masses $M \approx 10^6\ M_\odot$ and to turn on their radiation field at a redshift $z = 30$. By a detailed numerical modeling of nonequilibrium radiative transfer, we find that the typical size of the dissociated region is $R_d \approx 1$–$5$ kpc, while the ionization radius is about 3.5 times smaller; this result is in good agreement with the analytical estimate of equation (3). The mean distance between Population IIIs at $z \approx 20$–$30$ in a CDM model, $d \approx 0.01$–$1$ Mpc, is larger than $R_d$. Thus, at high redshift, the photodissociated regions are not large enough to overlap. In the same redshift range, the soft-UV background in the LW bands when the intergalactic H and $H_2$ opacity is included, is found to be $J_{LW} \approx 10^{-30}$ to $10^{-27}$ ergs cm$^{-2}$ s$^{-1}$ Hz$^{-1}$, depending on the star formation efficiency; this value is well below the threshold required for the negative feedback of Population III objects on the subsequent galaxy formation to be effective before redshift $\approx 20$.

T. A. acknowledges support from NASA grant NAG 5-3923. We thank F. Bertoldi, E. Corbelli, and P. Madau for useful discussions; M. Rees, N. Gnedin and the referee P. Shapiro for their stimulating comments.

## REFERENCES

Abel, T., Anninos, P., Zhang, Y., & Norman, M. L. 1997, NewA, 2, 181
Abgrall, H., & Roueff, E. 1989, A&AS, 79, 313
Anninos, P., & Norman, M. L. 1996, ApJ, 460, 556
Bond, J. R., Cole, S., Efstathiou, G., & Kaiser, N. 1991, ApJ, 379, 440
Bruzual, A. G., & Charlot, S. 1993, ApJ, 405, 538 (BC)
Ciardi, B., & Ferrara, A. 1997, ApJ, 483, L5
Copi, C. J., Schramm, D. N., & Turner, M. S. 1995, Science, 267, 192
Cowie, L. L., & Songaila, A. 1998, Nature, 344, 44
Cowie, L. L., Songaila, A., Kim, T. S., & Hu, E. M. 1995, AJ, 109, 1522
Dove, J. B., & Shull, J. M. 1994, ApJ, 423, 196
Draine, B. T., & Bertoldi, F. 1996, ApJ, 468, 269
Ferrara, A. 1998, ApJ, 499, L17
Ferrara, A., & Giallongo, E. 1996, MNRAS, 282, 1165
Giroux, M. L., & Shull, J. M. 1997, AJ, 113, 150
Gunn, J. E., & Peterson, B. A. 1965, ApJ, 142, 1633
Haiman, Z., Rees, M. J., & Loeb, A. 1997a, ApJ, 476, 458 (HRL)
———. 1997b, ApJ, 484, 985 (erratum, 476, 458)
Haiman, Z., Thoul, A. A., & Loeb, A. 1996, ApJ, 464, 523

Hurwitz, M., Jelinsky, P., & Dixon, W. V. 1997, ApJ, 481, L31
Leitherer, C., Ferguson, H. C., Heckman, T. M., & Lowental, J. D. 1995, ApJ, 454, L19
Lepp, S., & Shull, J. M. 1984, ApJ, 280, 465
Lu, L., Sargent, W. L. W., Barlow, T. A., & Rauch, M. 1998, preprint (astro-ph/9802189)
Madau, P. 1998, preprint (astro-ph/9804280)
Miralda-Escudé, J. 1997, preprint (astro-ph/9708253)
Osterbrock, D. E., Miller, D., & Joseph, S., eds. 1989, IAU Symp. 134, Astrophysics of Gaseous Nebulae and Active Galactic Nuclei (Mill Valley: University Science)
Palla, F., Galli, D., & Silk, J. 1995, ApJ, 451, 44
Peebles, P. J. E., & Dicke, R. H. 1968, ApJ, 154, 891
Press, W. H., & Schechter, P. 1974, ApJ, 187, 425
Savaglio, S., et al. 1997, A&A, 318, 347
Schmidt, M., Schneider, D. P., & Gunn, J. E. 1995, AJ, 110, 68
Shapiro, P. R. 1992, in IAU Symp. 150, Astrochemistry of Cosmic Phenomena, ed. P. D. Singh (Dordrecht: Kluwer Academic), 73
———. 1995, in ASP Conf. Ser. 80, The Physics of the Interstellar Medium and the Intergalactic Medium, ed. A. Ferrara et al. (San Francisco: ASP), 55
Shapiro, P. R., & Giroux, M. L. 1987, ApJ, 321, L107
Shapiro, P. R., Giroux, M. L., & Babul, A. 1994, ApJ, 427, 25
Shapiro, P. R., Giroux, M. L., & Kang, H. 1987, in High Redshift and Primeval Galaxies, ed. J. Bergeron et al. (Paris: Edition Frontières), 501
Shaver, P. A., et al. 1996, Nature, 384, 439
Tegmark, M., Silk, J., & Blanchard, A. 1994, ApJ, 420, 484
Tegmark, M., et al. 1997, ApJ, 474, 1
Tytler, D., et al. 1995, in QSOs Absorption Lines, Proc. ESO Workshop, ed. G. Meylan (Heidelberg: Springer), 289
Warren, S. J., Hewett, P. C., & Osmer, P. S. 1994, ApJ, 421, 412
White, S. D. M., & Frenk, C. S. 1991, ApJ, 379, 52